Author Manuscript

Author Manuscript

Author Manuscript

Author Manuscript

HHS Public Access

Author manuscript

J Am Chem Soc. Author manuscript; available in PMC 2021 January 04.

Published in final edited form as:

J Am Chem Soc. 2016 July 20; 138(28): 8802–8808. doi:10.1021/jacs.6b03681.

A Photoisomerizing Rhodopsin Mimic Observed at Atomic Resolution

Meisam Nosrati, **Tetyana Berbasova**, **Chrysoula Vasileiou**, **Babak Borhan***, **James H. Geiger***

Department of Chemistry, Michigan State University, East Lansing, Michigan 48824, United States

Abstract

The members of the rhodopsin family of proteins are involved in many essential light-dependent processes in biology. Specific photoisomerization of the protein-bound retinylidene PSB at a specified wavelength range of light is at the heart of all of these systems. Nonetheless, it has been difficult to reproduce in an engineered system. We have developed rhodopsin mimics, using intracellular lipid binding protein family members as scaffolds, to study fundamental aspects of protein/chromophore interactions. Herein we describe a system that specifically isomerizes the retinylidene protonated Schiff base both thermally and photochemically. This isomerization has been characterized at atomic resolution by quantitatively interconverting the isomers in the crystal both thermally and photochemically. This event is accompanied by a large pK_a change of the imine similar to the pK_a changes observed in bacteriorhodopsin and visual opsins during isomerization.

Graphical Abstract

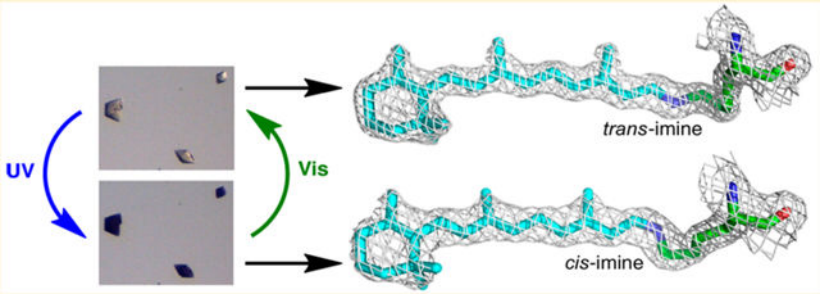

* **Corresponding Authors:** babak@chemistry.msu.edu, geiger@chemistry.msu.edu.

Supporting Information

The Supporting Information is available free of charge on the ACS Publications websiteat DOI: 10.1021/jacs.6b03681.

Experimental details for isomerization, UV–vis spectra, crystallization conditions, and X-ray data collection and refinement statistics. Crystallography, atomic coordinates and structure factors have been deposited in the Protein Data Bank, www.pdb.org (PDB ID codes: 4YBP, 4YBU, 4YCE, 4YCH, 4YDA, 4YDB, 4YFP, 4YFQ, 4YFR, 4YGG, 4YGH, 4YGZ, 4YH0, 4YKM, and 4YKO) (PDF)

The authors declare no competing financial interest.

Author Manuscript Author Manuscript Author Manuscript Author Manuscript

INTRODUCTION

Isomerization of the retinal chromophore is the key event in a variety of biological processes,[1] particularly those that involve visual perception,[2] circadian rhythm,[3] channeling ions across a membrane, light-induced phototaxis and signaling.[4] Additionally, photoisomerization of retinal, coupled to the action of channel rhodopsin and halorhodopsin to trigger light-dependent ion transport in neurons, has been exploited in the burgeoning field of optogenetics.[5] Rhodopsins bind an isomer of retinal as a protonated Schiff base (PSB, iminium) using a nucleophilic lysine residue in their binding pocket. Though they have a variety of biochemical activities, most share some common themes that are critical to their function. First they are characterized by a specific light induced *cis–trans* isomerization of the retinylidene moiety; usually either an 11-*cis* retinylidene isomerization in eukaryotic opsins (type II rhodopsins) or a 13-*cis* retinylidene isomerization in microbial rhodopsins (type I rhodopsins).[1] This specific isomerization is distinct from the behavior of retinylidene PSBs in solution, which gives mixtures of isomers upon irradiation. This isomerization places the retinylidene Schiff base (SB) in two distinct, local environments, directly affecting the pK_a of the imine functionality. For example, in microbial rhodopsins the isomerization of the C13 double bond results inasmuch as a 5–6 unit change in the pK_a of the protein-bound iminium.[6] In the rhodopsin visual pigment, this difference increases to 8–11 pK_a units.[7] Deprotonation of the PSB to a Schiff base (SB, imine) leads to a large shift in the absorption spectrum of the polyene from the visible region to the ultraviolet.[1] Although, the past two decades have witnessed a great deal of progress in understanding the mechanism of photoisomerization in different rhodopsins,[1,8] there are significant challenges in taming the isomerization process such that it is observable in real time, with structurally informative techniques. To the best of our knowledge, there are no reports that show complete photoisomerization of rhodopsin in the crystalline form,[9] and in bacteriorhodopsin, there is controversy regarding the structure of the intermediates identified spectroscopically.[10] A model system that is able to reproduce an isomerization event in a controlled manner would allow a much more detailed examination of these processes. Herein, we demonstrate the first steps toward this goal.

Our work has focused on the development of soluble, easily manipulated rhodopsin mimics derived from the reengineering of cellular retinoid binding proteins that belong to the intracelluar lipid binding family of proteins (iLBP),[11] namely human cellular retinol binding protein II (hCRBPII)[12] and human cellular retinoic acid binding protein II (CRABPII).[13] We have used these systems to unravel the mechanism of wavelength tuning, where the protein environment alters the absorption properties of a bound chromophore over a wide wavelength range. This has culminated in the development of a set of retinal-bound proteins with absorption maxima that range from 425 to 644 nm,[12a,13e] more than 50 nm further than any of the natural rhodopsin systems. These studies have shed light on the fundamental mechanisms of protein-based wavelength tuning, with potential applications in a wide range of systems. The reengineered iLBPs have also shown a great deal of potential as fluorescent protein tags and also pH responsive reporters.[13e,14] With respect to the latter, we have had the good fortune of identifying mutants of CRABPII and hCRBPII that can interconvert between two putatively isomeric states either thermally or photochemically.[13e,15] Such a

Author Manuscript Author Manuscript Author Manuscript Author Manuscript

system could provide a natural laboratory for the study of the basic photophysics of the rhodopsins and also create a platform for the development of novel photoswitchable proteins for use in a variety of applications, including photoswitchable fluorescent or fluorescence quenching proteins. In the past few years the discovery of reversibly switchable fluorescent proteins (RSFPs) that can be switched between fluorescent and nonfluorescent states has enabled the development of numerous high- and super-resolution microscopy and imaging techniques.[16]

Our efforts in developing light responsive proteins have resulted in the design and demonstration of a robust photoswitchable rhodopsin mimic through the reengineering of CRABPII. Further, we have characterized the two photoswitchable forms as the 15-*cis* and -*trans* retinylidene protein-bound isomers by UV–vis spectroscopy and X-ray crystallography. The well-behaved nature of these proteins has led, for the first time, to a system capable of quantitative, reversible photoisomerization in single crystals over several isomerization cycles. The elucidated structures unequivocally reveal the isomeric forms for both photostates at high resolution, making this one of the best characterized photoswitchable protein systems known so far.

RESULTS AND DISCUSSION

We recently demonstrated photoinduced changes in the protonation state of a retinylidene bound mutant of CRABPII.[15] Based on the spectroscopic changes observed during photoirradiation, we hypothesized that the change in the protonation state of the imine functionality (either protonated as a colored iminium, or deprotonated as a colorless imine) was likely due to the light-triggered isomerization of the chromophore. Nonetheless, verification of this hypothesis, and the precise identification of the two photoisomers, is best obtained from high-resolution structural data. After many trials, it became clear that a new set of mutants with appropriate imine pK_a, faster rates of chromophore binding, and improved photochemical characteristics are required to obtain the necessary crystallographic evidence. Even more ambitiously, we hoped to create a system that would photochemically isomerize reversibly in the solid state, without loss of crystalline order. For this purpose, CRABPII was used as a template to design a photoactive version of a rhodopsin mimic. As previously described,[13e] four mutations were required to obtain an optimal CRABPII mutant that would bind retinal and react to form a stable PSB. The R111K mutation provides the nucleophile for PSB formation, while the R132L, Y134F, and T54V mutations were required to remove the original retinoid binding site and facilitate the formation of the requisite iminium. The resulting R111K:R132L:Y134F:T54V tetra mutant (KLFV) provides a starting template for further alterations.

The design of a functioning photoswitchable mimic of rhodopsin requires that a single photoisomerization event results in a substantial change in the pK_a of the retinal PSB. This would lead to a simple visual readout since the PSB, strongly colored due to the protonation of the imine, would lose absorption in the visible spectrum upon deprotonation. To this end, we sought to increase the iminium pK_a of the CRABPII rhodopsin mimics. This was achieved by placing two critical Gln residues in the vicinity of the bound chromophore to aid in increasing the binding pocket’s overall hydrophilicity. The sites for introduction of the

Author Manuscript Author Manuscript Author Manuscript Author Manuscript

Gln residues were identified through comparison of the CRABPII sequence with hCRBPII mutants that had previously demonstrated high pK_a (Figure 1). In addition, mutation of Arg59 to Tyr was instrumental in gaining higher pK_a.[12a] The culmination of these changes led to the R111K:Y134F:T54V:R132Q:P39Q:R59Y (**M1**) CRABPII hexamutant. Interestingly, base titration of **M1** complexed with retinal as a PSB revealed a broad transition, ranging from pH of 4.3 to 10.5, which is inconsistent with the behavior of a weak acid/base system with a single pK_a. P39Q and R132Q mutations gave similar results (see Figure S1).

A possible explanation for this behavior came from our previous studies of retinal-bound CRABPII mutants, where we had observed the conversion of the PSB to the SB (loss of the iminium proton) in a time scale ranging from minutes to hours. We discovered that these proteins convert from a high pK_a to much lower pK_a form, suggesting a change of environment in the vicinity of the iminium nitrogen atom as the culprit.[13e] We had hypothesized that the change in the environment could be attributed to an isomerization of one of the double bonds in the chromophore, analogous to that seen in the natural rhodopsin systems.[1] Similar to the mutants described above, **M1** also converts over time from a higher to a lower pK_a form, however, the rate of interconversion between the two forms is substantially slower than that seen in previous mutants (Figure 2a). We surmised that the reduced rate of interconversion might allow for the trapping and unequivocal identification of each form crystallographically. It is important to note that **M1** was substantially slower in forming the initial PSB, requiring nearly 4 h to achieve maximum levels of PSB formation.

To identify the final, SB product, crystallization of **M1** commenced only after all of the PSB had disappeared (24 h). This resulted in a clear electron density map consistent with an all *trans* configuration for all the chromophore's double bonds, including the iminium (Figure 2b). Attempts at trapping the high pK_a form of **M1**, by initiating crystallization trials immediately after PSB formation, resulted in crystals with ambiguous electron density for the chromophore, especially in the vicinity of the iminium region. There are two potential problems with this approach. First and most obvious is that partial conversion may occur before crystal nucleation, resulting in an ambiguous mixture of the two isomeric forms. Second, the comparatively long incubation time required for the PSB to fully form (4 h) could result in a situation where the metastable form is never the exclusive form in solution. To overcome this, we aimed to significantly accelerate the formation of the PSB, such that the initial high pK_a species is fully formed before it has time to significantly isomerize.

Fortuitously, our screening of position 39 led to mutants that exhibited the necessary rate acceleration in PSB formation of the protein complexed with retinal and yet maintained the desired pK_a difference between the two putative isomeric forms (See Table S1 for a summary of mutants). In particular, R111K:R134F:T54V:R132Q:P39Y:R59Y (**M2**) yielded the fully formed PSB in 20 min, followed by a slow conversion to the SB (over 10 h, Figure 3a). Crystallization trials of retinal-bound **M2** were initiated both 20 min and 24 h after retinal addition. Gratifyingly, the electron density produced from crystals grown after short retinal incubation clearly showed the presence of a *cis*-imine bond, while crystals grown from protein incubated with retinal for 24 h produced electron density that was unambiguously that of a *trans*-imine (Figure 3b,c). These results suggest that crystal

Author Manuscript Author Manuscript Author Manuscript Author Manuscript

formation occurs rapidly, allowing the less stable *cis*-imine to nucleate before significant amounts of the *trans* isomer have formed.

The **M2** mutant resembles a functional rhodopsin mimic in that it can interconvert via chromophore isomerization and place the imine in two distinct environments that substantially alter its pK_a. Nonetheless, the key property of such a system is that it must be photoswitchable. The **M2** protein has a low pK_a (3.4) for its 15-*trans* SB form with absorption in the UV region (λ_{max} = 370 nm), while the 15-*cis* high pK_a species (8.2) has a strong absorption band in the visible region (λ_{max} = 571 nm). The protein complex with its fully maximized PSB absorption was irradiated using visible yellow light for 1 min (see SI for details of light irradiation protocols). This led to a complete loss of the PSB peak, with the concomitant rise of the SB absorption at 370 nm, which we now know is the result of the photoisomerization of the *cis* imine to the *trans* isomer. The original *cis*-imine state, with the PSB absorption in the visible region, was regenerated upon photoirradiation of the latter solution with UV light. The photoinduced interconversion of the two isomeric states was repeated several times, illustrating the reversibility of the protein/chromophore complex with excellent fatigue resistance (Figure S5).

Having shown that light irradiation of **M2** interconverts its two isomeric states in solution, we explored the feasibility of the same process occurring in the crystalline state. The crystals of retinal-bound **M2**, grown after 24 h of incubation and soaked in a pH 7.5 stabilizer, were essentially colorless since the *trans*-imine isomer (Figure 4a), with its low pK_a, has minimal absorption in the visible spectrum. Exposure of these crystals to UV light resulted in an intense purple color within 1 min of irradiation. Visible light irradiation regenerated the colorless crystals. As depicted in Figure 4b, this process was repeated several times without any visible damage to the crystals. The change of absorption in the solid state suggests the isomerization of the *cis*-iminium to the *trans*-imine, and vice versa. The loss and gain of color is indicative of the change in the pK_a of the imine nitrogen and the protonation state of the Schiff base. This was in fact verified by solving the structures of the crystals after photoisomerization with UV and also visible light to demonstrate that the changes in the imine geometry go along with the observed changes in the pK_a. The crystal structures from the first two steps of the irradiation cycle are depicted in Figure 4c, while the data for cycles thereafter are tabulated in Tables S2 and S3. Of note, the overlay of the metastable *cis*-PSB structure obtained by immediate crystallization after PSB formation and the UV irradiated crystal structure shows the two to be essentially identical, while the low pK_a *trans*-SB structure is distinctly different (Figure 4c). Similarly, the crystal structures from the thermally matured sample were identical to those obtained from the visible light irradiation of the colored crystals that reveal the *trans*-SB isomer (Figure S10). It is important to note that the imine geometry dictates the orientation and trajectory of the lysine side chain. As seen in Figure 4c, the change in the side chain trajectory is directly correlated to the imine isomer and thus can be used as corroborating evidence for establishing the imine geometry.

The overlay of the two isomeric forms of **M2** indicates that the position and orientation of critical residues surrounding the chromophore, and the chromophore itself, are unchanged, (Figure 5a). The only noticeable movement of the residues inside the binding pocket involves Leu121. In the *trans*-SB form, this residue has enough space to adopt two different

Author Manuscript Author Manuscript Author Manuscript Author Manuscript

conformations. As the lysine moves out in the *cis*-PSB form, one of the conformations of Leu121 becomes disfavored due to steric hindrance (Figure 5a). Nonetheless, the most drastic difference is in the trajectory of Lys111, which forms the imine. The structure of the *cis*-imine isomer reveals the protonated nitrogen atom to be 3–3.5 Å away from Trp109, close enough to make a strong π–cation interaction, presumably aiding in the stabilization of the protonated species (Figure 5b). Conversely, the imine in the *trans* isomer is surrounded by hydrophobic residues (Val41, Ile43, Leu119, and Leu121) that lead to a severely depressed pK_a (Figure 5c). The change in the imine environment, and thus the acidity of the SB, mimics the process postulated in rhodopsin and bacteriorhodopsin. One can, therefore, propose that the change in the pK_a is tunable as a function of environmental factors. Indeed, with the few case studies here, the trend does hold. For example, mutants that contain the R132Q:P39Q modification exhibit a 2–3 pK_a unit change between the 15-*cis* and 15-*trans* forms. This difference can be accentuated to 5 units in CRABPII/chromophore complexes that contain the R132Q:P39Y mutation.

The photocycle depicted in Figure 6 was suggested previously to explain the UV–vis spectra for several other photoirradiated CRABPII mutants.[15] At this juncture, the spectroscopic and crystallographic data provide a solid foundation for this proposal. Starting with a *cis*-PSB as the initial kinetic form of the protein/chromophore complex, a thermal isomerization to the *trans*-SB form reduces the pK_a of the imine below physiological pH, resulting in the observed blue shift that yields a colorless system. The same thermal process can be greatly accelerated by green light irradiation. Regeneration of the initial isomeric form (*cis*-imine) is only possible photochemically through UV irradiation of the thermodynamic *trans*-imine complex. This cycle can be repeated without significant loss of intensity, both in solution and in the crystal form of the complex.

As compared to all the natural rhodopsins, our engineered system seems most similar to the *Anabaena* sensory rhodopsin (ASR).[17] Both systems involve iminium photoisomerization, though in ASR, both the 13 and 15 double bonds isomerize, while in our system only the iminium isomerizes. In addition, both systems are photochromic, meaning that there are two stable forms of the chromophore and both undergo photo-isomerization. Understanding in detail the photocycle of our engineered system awaits time-resolved spectroscopic investigation.

In a final demonstration of environmental factors affecting isomeric distribution and imine acidity, we looked to engineer an analogous protein/chromophore complex that would thermodynamically favor the *cis*-PSB form as opposed to the systems discussed thus far that favor the *trans*-SB isomer. Extrapolating from over 50 crystal structures of CRABPII and hCRBPII mutants investigated during the course of wavelength regulation studies, we noted a common occurrence; namely, the presence of a Gln residue at position 3 (residue 4 for hCRBPII) yields crystal structures with a *cis*-imine configuration, while other mutations of this residue most often provide the *trans*-SB.[12a] Analogously, the R111K:Y134F:T54V:R132Q:P39Q:-R59Y:A32W:F3Q mutant (**M3**) was prepared, yielding a protein/chromophore complex that exhibited high PSB stability (50% of the PSB present after 24 h). Predictably, photoirradiation of **M3** with visible light results in the loss of the PSB absorbance with a concomitant increase in the intensity of the SB peak. In contrast to

Author Manuscript Author Manuscript Author Manuscript Author Manuscript

other systems discussed here, the color of the complex recovers in darkness, indicating thermal isomerization to the higher pK_a, presumably *cis*-PSB form (Figures S5 and S6). Crystals of **M3** do indeed corroborate the latter statement, consistent with the extensive stabilization of the *cis* form conferred by the F3Q mutation (Figure 7). Attempts to photoisomerize **M3** crystals in the solid state were not fruitful.

CONCLUSION

Using a rational design strategy based on the CRABPII scaffold, we have created a series of rhodopsin mimics that reproduce the basic chemistry in these systems, in that photoisomerization switches the retinal iminium between two distinct pK_a regimes. We have further demonstrated the ability to independently control both pK_as and alter the thermal product from the low to the high pK_a moiety. Both forms have been unambiguously identified from high-resolution crystal structures, and photoisomerization in the crystalline state was also demonstrated, with quantitative conversion between each form shown at atomic resolution. This represents a fully engineered retinal-based photoswitchable protein that has a variety of potential applications. The quantitative photoisomerization in the crystal makes this a potentially ideal system for time-resolved crystallographic experiments. Modification of the retinal chromophore to a fluorescent derivative could yield photoswitchable fluorescent proteins, useful in a variety of applications.

Supplementary Material

Refer to Web version on PubMed Central for supplementary material.

ACKNOWLEDGMENTS

This work was funded by the NIH (grant no. GM101353). The crystallography data for all the structures were collected at Advanced Photon Source, an Office of Science User Facility operated for the U.S. Department of Energy (DOE) Office of Science by Argonne National Laboratory, supported by the U.S. DOE under contract no. DE-AC02-06CH11357. Use of the LS-CAT Sector 21 was supported by the Michigan Economic Development Corporation and the Michigan Technology Tri-Corridor (grant 085P1000817).

REFERENCES

(1). Ernst OP; Lodowski DT; Elstner M; Hegemann P; Brown LS; Kandori H Chem. Rev 2014, 114, 126. [PubMed: 24364740]

(2). (a)Bowmaker JK; Dartnall HJA J. Physiol. (Oxford, U. K.) 1980, 298, 501.(b)Palczewski K Annu. Rev. Biochem 2006, 75, 743. [PubMed: 16756510] (c)Palczewski K; Kumasaka T; Hori T; Behnke CA; Motoshima H; Fox BA; Le Trong I; Teller DC; Okada T; Stenkamp RE; Yamamoto M; Miyano M Science 2000, 289, 739. [PubMed: 10926528]

(3). (a)Matsuyama T; Yamashita T; Imamoto Y; Shichida Y Biochemistry 2012, 51, 5454. [PubMed: 22670683] (b)Rinaldi S; Melaccio F; Gozem S; Fanelli F; Olivucci M Proc. Natl. Acad. Sci. U. S. A 2014, 111, 1714. [PubMed: 24449866] (c)Walker MT; Brown RL; Cronin TW; Robinson PR Proc. Natl. Acad. Sci. U. S. A 2008, 105, 8861. [PubMed: 18579788]

(4). (a)Choe HW; Park JH; Kim YJ; Ernst OP Neuropharmacology 2011, 60, 52. [PubMed: 20708633] (b)Choe HW; Kim YJ; Park JH; Morizumi T; Pai EF; Krauss N; Hofmann KP; Scheerer P; Ernst OP Nature 2011, 471, 651. [PubMed: 21389988] (c)Gordeliy VI; Labahn J; Moukhametzianov R; Efremov R; Granzin J; Schlesinger R; Buldt G; Savopol T; Scheidig AJ; Klare JP; Engelhard M Nature 2002, 419, 484. [PubMed: 12368857] (d)Fu HY; Lin YC; Chang YN; Tseng H; Huang

Author Manuscript Author Manuscript Author Manuscript Author Manuscript

CC; Liu KC; Huang CS; Su CW; Weng RR; Lee YY; Ng WV; Yang CS J. Bacteriol 2010, 192, 5866. [PubMed: 20802037]

(5). (a)Warden MR; Cardin JA; Deisseroth K Annu. Rev. Biomed. Eng 2014, 16, 103. [PubMed: 25014785] (b)Yizhar O; Fenno LE; Davidson TJ; Mogri M; Deisseroth K Neuron 2011, 71, 9. [PubMed: 21745635]

(6). (a)Sheves M; Albeck A; Friedman N; Ottolenghi M Proc. Natl. Acad. Sci. U. S. A 1986, 83, 3262. [PubMed: 3458179] (b)Rousso I; Friedman N; Sheves M; Ottolenghi M Biochemistry 1995, 34, 12059. [PubMed: 7547944] (c)Brown LS; Lanyi JK Proc. Natl. Acad. Sci. U. S. A 1996, 93, 1731. [PubMed: 8643698]

(7). (a)Steinberg G; Ottolenghi M; Sheves M Biophys. J 1993, 64, 1499. [PubMed: 8391868] (b)Mahalingam M; Vogel R Biochemistry 2006, 45, 15624. [PubMed: 17176084] (c)Bartl FJ; Vogel R Phys. Chem. Chem. Phys 2007, 9, 1648. [PubMed: 17396175]

(8). (a)Frutos LM; Andruniow T; Santoro F; Ferre N; Olivucci M Proc. Natl. Acad. Sci. U. S. A 2007, 104, 7764. [PubMed: 17470789] (b)Gozem S; Schapiro I; Ferre N; Olivucci M Science 2012, 337, 1225. [PubMed: 22955833] (c)Kukura P; McCamant DW; Yoon S; Wandschneider DB; Mathies RA Science 2005, 310, 1006. [PubMed: 16284176] (d)Polli D; Altoe P; Weingart O; Spillane KM; Manzoni C; Brida D; Tomasello G; Orlandi G; Kukura P; Mathies RA; Garavelli M; Cerullo G Nature 2010, 467, 440. [PubMed: 20864998]

(9). (a)Nakamichi H; Okada T Angew. Chem., Int. Ed 2006, 45, 4270.(b)Nakamichi H; Okada T Proc. Natl. Acad. Sci. U. S. A 2006, 103, 12729. [PubMed: 16908857]

(10). (a)Borshchevskiy VI; Round ES; Popov AN; Buldt G; Gordeliy VI J. Mol. Biol 2011, 409, 813. [PubMed: 21530535] (b)Lanyi JK; Schobert B J. Mol. Biol 2007, 365, 1379. [PubMed: 17141271] (c)Matsui Y; Sakai K; Murakami M; Shiro Y; Adachi S; Okumura H; Kouyama T J. Mol. Biol 2002, 324, 469. [PubMed: 12445782]

(11). (a)Banaszak L; Winter N; Xu ZH; Bernlohr DA; Cowan S; Jones TA Adv. Protein Chem 1994, 45, 89. [PubMed: 8154375] (b)Bernlohr DA; Simpson MA; Hertzel AV; Banaszak LJ Annu. Rev. Nutr 1997, 17, 277. [PubMed: 9240929] (c)Coe NR; Bernlohr DA Biochim. Biophys. Acta, Lipids Lipid Metab 1998, 1391, 287.

(12). (a)Wang WJ; Nossoni Z; Berbasova T; Watson CT; Yapici I; Lee KSS; Vasileiou C; Geiger JH; Borhan B Science 2012, 338, 1340. [PubMed: 23224553] (b)Wang W; Geiger JH; Borhan B BioEssays 2014, 36, 65. [PubMed: 24323922]

(13). (a)Crist RM; Vasileiou C; Rabago-Smith M; Geiger JH; Borhan B J. Am. Chem. Soc 2006, 128, 4522. [PubMed: 16594659] (b)Vasileiou C; Vaezeslami S; Crist RM; Rabago-Smith M; Geiger JH; Borhan B J. Am. Chem. Soc 2007, 129, 6140. [PubMed: 17447762] (c)Vasileiou C; Lee KSS; Crist RM; Vaezeslami S; Goins SA; Geiger JH; Borhan B Proteins: Struct., Funct., Genet 2009, 76, 281. [PubMed: 19156818] (d)Vasileiou C; Wang WJ; Jia XF; Lee KSS; Watson CT; Geiger JH; Borhan B Proteins: Struct., Funct., Genet 2009, 77, 812. [PubMed: 19603486] (e)Berbasova T; Nosrati M; Vasileiou C; Wang WJ; Sing K; Lee S; Yapici I; Geiger JH; Borhan B J. Am. Chem. Soc 2013, 135, 16111. [PubMed: 24059243] (f)Lee KSS; Berbasova T; Vasileiou C; Jia XF; Wang WJ; Choi Y; Nossoni F; Geiger JH; Borhan B ChemPlusChem 2012, 77, 273.

(14). Yapici I; Lee KS; Berbasova T; Nosrati M; Jia X; Vasileiou C; Wang W; Santos EM; Geiger JH; Borhan B J.Am. Chem. Soc 2015, 137, 1073. [PubMed: 25534273]

(15). Berbasova T; Santos EM; Nosrati M; Vasileiou C; Geiger JH; Borhan B ChemBioChem 2016, 17, 407. [PubMed: 26684483]

(16). (a)Duan CX; Adam V; Byrdin M; Ridard J; Kieffer-Jaquinod S; Morlot C; Arcizet D; Demachy I; Bourgeois D J. Am. Chem. Soc 2013, 135, 15841. [PubMed: 24059326] (b)Tiwari DK; Nagai T Dev. Growth Differ 2013, 55, 491. [PubMed: 23635320] (c)Nienhaus K; Ulrich Nienhaus G Chem. Soc. Rev 2014, 43, 1088. [PubMed: 24056711] (d)Shcherbakova DM; Subach OM; Verkhusha VV Angew. Chem., Int. Ed 2012, 51, 10724.(e)Andresen M; Stiel AC; Trowitzsch S; Weber G; Eggeling C; Wahl MC; Hell SW; Jakobs S Proc. Natl. Acad. Sci. U. S. A 2007, 104, 13005. [PubMed: 17646653] (f)Henderson JN; Ai HW; Campbell RE; Remington SJ Proc. Natl. Acad. Sci. U. S. A 2007, 104, 6672. [PubMed: 17420458] (g)Andresen M; Wahl MC; Stiel AC; Grater F; Schafer LV; Trowitzsch S; Weber G; Eggeling C; Grubmuller H; Hell SW; Jakobs S Proc. Natl. Acad. Sci. U. S. A 2005, 102, 13070. [PubMed: 16135569] (h)Brakemann T; Stiel

Author Manuscript Author Manuscript Author Manuscript Author Manuscript

AC; Weber G; Andresen M; Testa I; Grotjohann T; Leutenegger M; Plessmann U; Urlaub H; Eggeling C; Wahl MC; Hell SW; Jakobs S Nat. Biotechnol 2011, 29, 942. [PubMed: 21909082]

(17). (a)Kawanabe A; Furutani Y; Jung KH; Kandori H J. Am. Chem. Soc 2007, 129, 8644. [PubMed: 17569538] (b)Strambi A; Durbeej B; Ferre N; Olivucci M Proc. Natl. Acad. Sci. U. S. A 2010, 107, 21322. [PubMed: 21098308] (c)Vogeley L; Sineshchekov OA; Trivedi VD; Sasaki J; Spudich JL; Luecke H Science 2004, 306, 1390. [PubMed: 15459346]

Author Manuscript Author Manuscript Author Manuscript Author Manuscript

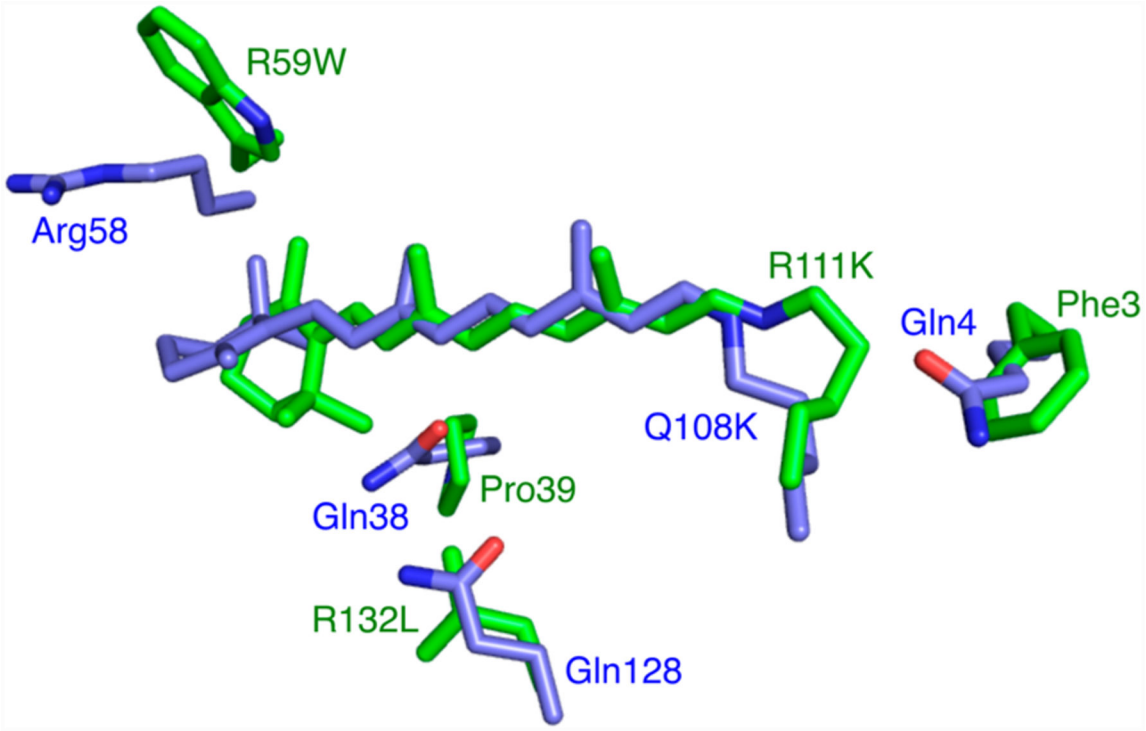

Figure 1.

Structures of the CRABPII mutant R111K:R132L:Y134F:T54V:R59W (green, PDB ID 4I9S) and the hCRBPII mutant Q108K:K40L (blue, PDB ID 4RUU) were overlaid, and the region around the retinal binding site is shown. Note the three glutamines in hCRBPII are substituted with hydrophobic residues in CRABPII, leading to a much higher pK_a for the former. Atoms, here and throughout, are colored as follows: O is red, N is blue, and C is green unless otherwise indicated.

Author Manuscript Author Manuscript Author Manuscript Author Manuscript

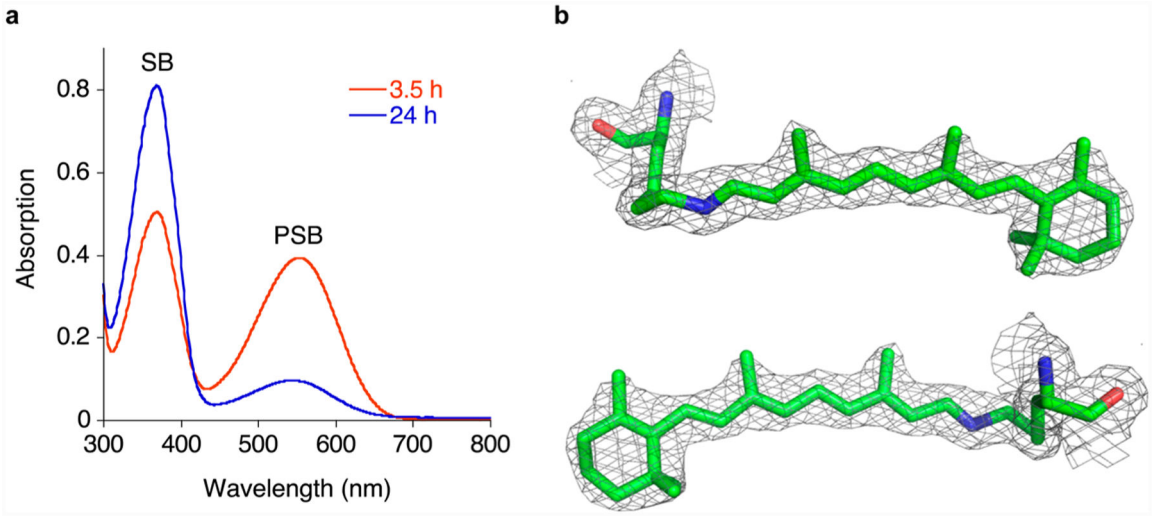

Figure 2.

Thermal conversion of the **M1** mutant. (a) UV–vis spectra of the **M1**/retinal complex 3.5 and 24 h after addition of retinal to the protein at physiological pH. (b) Two views (the bottom rotated 180° about a vertical axis relative to the top view) of the retinal density in the crystal structure of R111K:R134F:T54V:P39Q:R132Q:R59Y at 1.83 Å contoured at 1σ shows a *trans*-SB (PDB ID: 4YBP).

Author Manuscript Author Manuscript Author Manuscript Author Manuscript

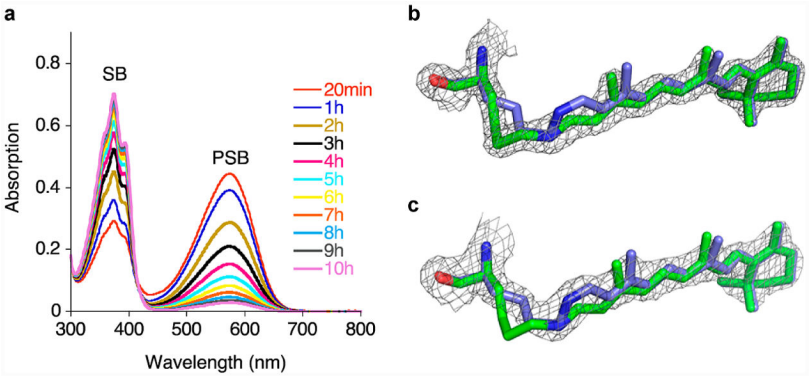

Figure 3.

Thermal isomerization of a CRABPII rhodopsin mimic. (a) PSB loss over time for the **M2** mutant. **M2** was incubated with retinal, and UV–vis spectra were taken at various time points. (b) Crystal structure of **M2** showing the *trans*-SB at 1.62 Å, with the electron density contoured at 2.0 σ, (green, protein was incubated with 4 equiv retinal for 24 h at room temperature before crystallization, PDB ID: 4YFQ), overlaid on the *cis*-PSB of the same mutant crystallized after 20 min of retinal incubation (blue). (c) Crystal structure of the **M2** mutant in *cis*-PSB form at 1.97 Å at 1.5 σ (blue, the protein was incubated with 4 equiv of retinal at room temperature for 20 min, followed by immediate crystallization, PDB ID: 4YFP) overlaid on the *trans*-SB of the same mutant (green).

Author Manuscript Author Manuscript Author Manuscript Author Manuscript

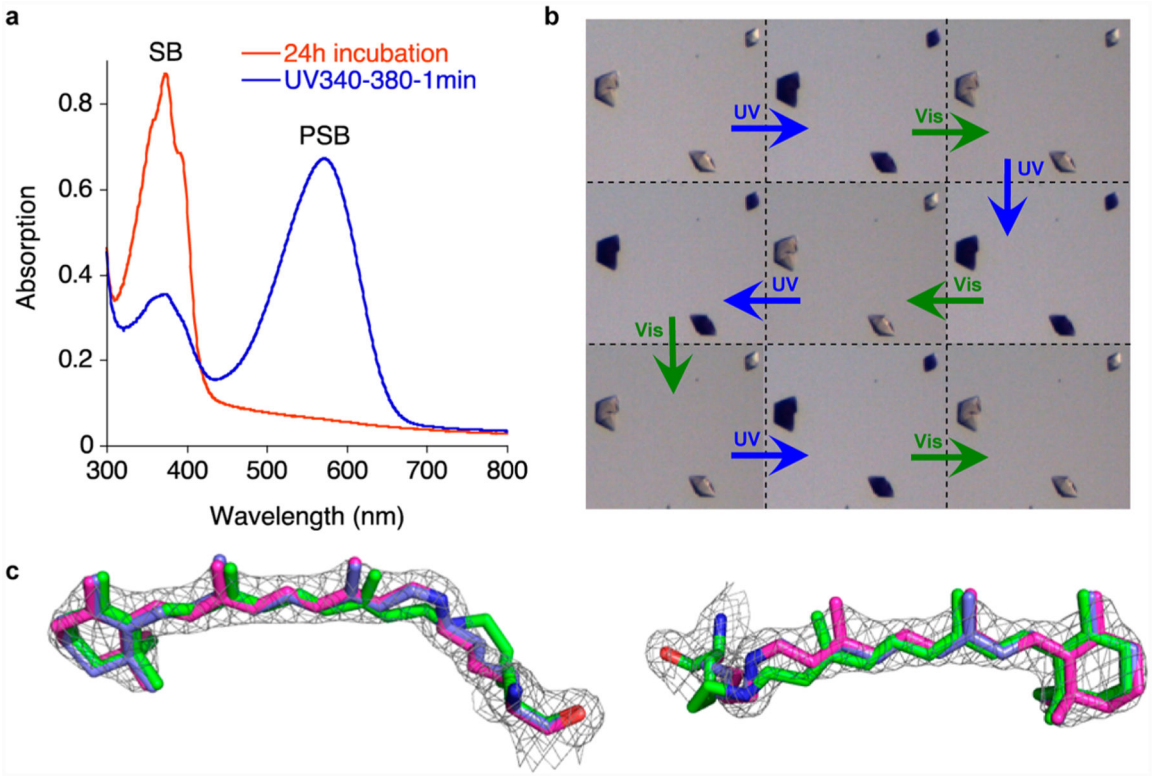

Figure 4.

Photointerconversion in both solution and crystalline state. (a) UV irradiation of **M2** (UV band-pass filter) after complete PSB loss (24 h incubation, red spectrum) shows the PSB recovery in solution (blue spectrum). (b) Cycles of UV and visible light irradiation of **M2** crystals (each cycle is 5 min UV light and 5 min white light irradiation at pH 7.5). (c) The structure of **M2** mutant (magenta, PDB ID: 4YFR, 1.95 Å resolution) obtained from a crystal that was UV irradiated for 30 min, overlaid with the metastable *cis*-PSB structure (blue, PDB ID: 4YFP, see text for description). The electron density was contoured at 1.5 σ; the structure clearly shows the bound retinal adopts a *cis* imine geometry; also overlaid is the crystal structure of the *trans*-SB (green, PDB ID: 4YFQ) to highlight the change in structure and its inability to fit the electron density obtained for the UV irradiated crystals. While the left view clearly shows the lysine side chain of the *trans* imine isomer is out of the density, the right view shows the motion of the retinal.

Author Manuscript Author Manuscript Author Manuscript Author Manuscript

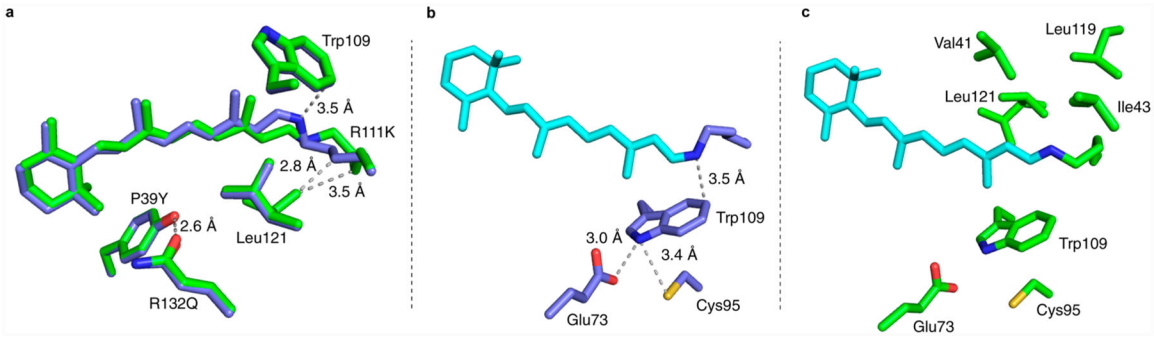

Figure 5.

M2 crystal structures of both imine isomers reveal differences that correlate the changes in the pK_a of the two isomeric forms of the protein to the environment of the imine functionality. (a) An overlay of the *cis*- (blue carbons) and *trans*- (green carbons) iminium retinylidene **M2** structures (PDB ID: 4YFP (blue) and 4YFQ (green). (b) The *cis-iminium* retinylidene **M2** structure. Note that a π–cation interaction between Trp109 and the PSB nitrogen of the *cis*-PSB contributes to the higher pK_a in this form (PDB ID: 4YFP). (c) Hydrophobic residues surrounding the *trans*-SB in **M2** depress the pK_a in this form (PDB ID: 4YFQ). Note that Leu121 has two conformations with nearly equal occupancies.

Author Manuscript Author Manuscript Author Manuscript Author Manuscript

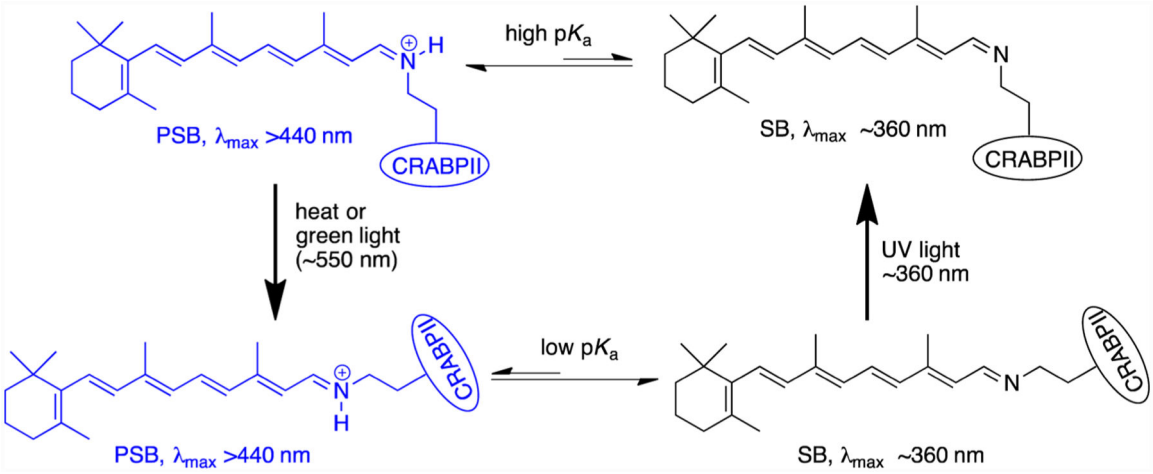

Figure 6.

Thermodynamic and light-induced *cis*, *trans*-retinal iminium isomerization in CRABPII protein.

Author Manuscript Author Manuscript Author Manuscript Author Manuscript

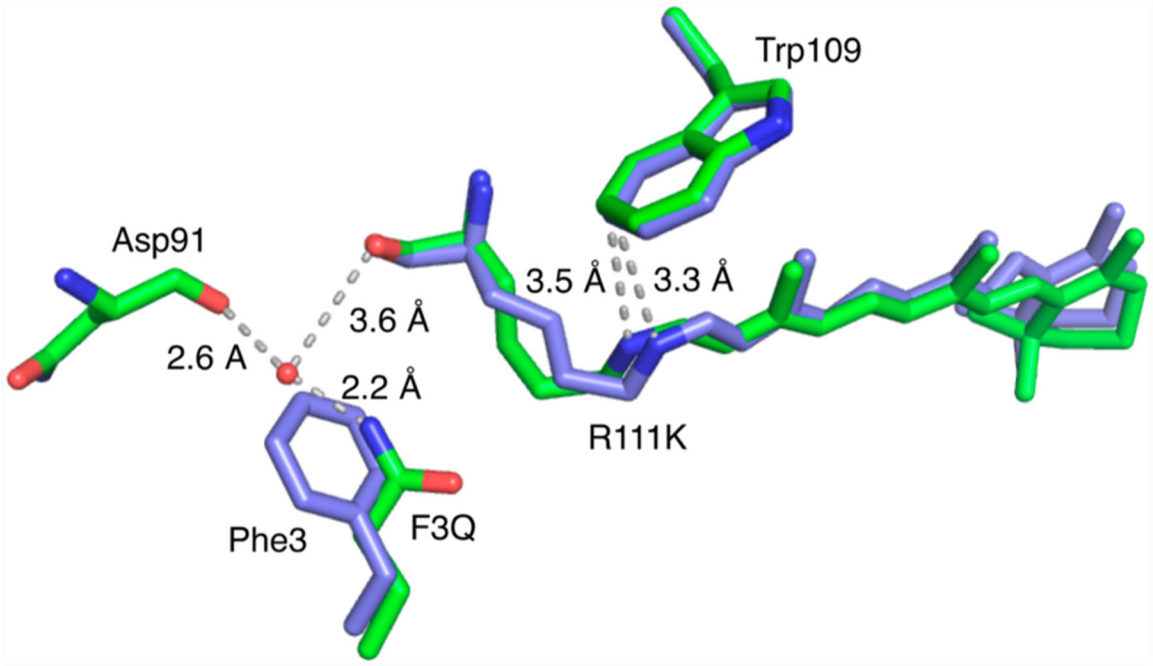

Figure 7.

Structures of retinal-bound **M3** (green) (PDB ID: 4YKM) and *cis*-PSB retinal-bound **M2** (blue) (PDB ID: 4YFP) are overlaid, showing the effect of F3Q on the environment near the *cis*-PSB, increasing the pK_a by 1 unit and altering the nature of the thermodynamic product.